



Latest updates: <https://dl.acm.org/doi/10.1145/3696410.3714782>

RESEARCH-ARTICLE

MedRAG: Enhancing Retrieval-augmented Generation with Knowledge Graph-Elicited Reasoning for Healthcare Copilot

XUEJIAO ZHAO, Nanyang Technological University, Singapore City, Singapore

SIYAN LIU, Nanyang Technological University, Singapore City, Singapore

SUYIN YANG, Tan Tock Seng Hospital, Singapore City, Singapore

CHUNYAN MIAO, Nanyang Technological University, Singapore City, Singapore

Open Access Support provided by:

Nanyang Technological University

Tan Tock Seng Hospital



PDF Download
3696410.3714782.pdf
05 January 2026
Total Citations: 29
Total Downloads: 5889

Published: 28 April 2025

Citation in BibTeX format

WWW '25: The ACM Web Conference

2025

April 28 - May 2, 2025

Sydney NSW, Australia

Conference Sponsors:
SIGWEB

MedRAG: Enhancing Retrieval-augmented Generation with Knowledge Graph-Elicited Reasoning for Healthcare Copilot

Xuejiao Zhao*

LILY Research Centre

Nanyang Technological University
Singapore
xjzhao@ntu.edu.sg

Su-Yin Yang

Tan Tock Seng Hospital
Woodlands Health
Singapore
su_yin_yang@wh.com.sg

Siyan Liu*

LILY Research Centre

Nanyang Technological University
Singapore
siyan.liu@ntu.edu.sg

Chunyan Miao†

LILY Research Centre
Nanyang Technological University
Singapore
ascymiao@ntu.edu.sg

Abstract

Retrieval-augmented generation (RAG) is a well-suited technique for retrieving privacy-sensitive Electronic Health Records (EHR). It can serve as a key module of the healthcare copilot, helping reduce misdiagnosis for healthcare practitioners and patients. However, the diagnostic accuracy and specificity of existing heuristic-based RAG models used in the medical domain are inadequate, particularly for diseases with similar manifestations. This paper proposes MedRAG, a RAG model enhanced by knowledge graph (KG)-elicited reasoning for the medical domain that retrieves diagnosis and treatment recommendations based on manifestations. MedRAG systematically constructs a comprehensive four-tier hierarchical diagnostic KG encompassing critical diagnostic differences of various diseases. These differences are dynamically integrated with similar EHRs retrieved from an EHR database, and reasoned within a large language model. This process enables more accurate and specific decision support, while also proactively providing follow-up questions to enhance personalized medical decision-making. MedRAG is evaluated on both a public dataset DDXPlus and a private chronic pain diagnostic dataset (CPDD) collected from Tan Tock Seng Hospital, and its performance is compared against various existing RAG methods. Experimental results show that, leveraging the information integration and relational abilities of the KG, our MedRAG provides more specific diagnostic insights and outperforms state-of-the-art models in reducing misdiagnosis rates. Our code will be available at <https://github.com/SNOWTEAM2023/MedRAG>

CCS Concepts

- Applied computing → Health care information systems; • Information systems → Language models.

*Both authors contributed equally to the paper

†Corresponding author



This work is licensed under a Creative Commons Attribution-NonCommercial-NoDerivatives 4.0 International License.

WWW '25, Sydney, NSW, Australia

© 2025 Copyright held by the owner/author(s).

ACM ISBN 979-8-4007-1274-6/25/04

<https://doi.org/10.1145/3696410.3714782>

Keywords

Healthcare Copilot, Retrieval-augmented Generation, Knowledge Graph, Large Language Models, Decision Support

ACM Reference Format:

Xuejiao Zhao, Siyan Liu, Su-Yin Yang, and Chunyan Miao. 2025. MedRAG: Enhancing Retrieval-augmented Generation with Knowledge Graph-Elicited Reasoning for Healthcare Copilot. In *Proceedings of the ACM Web Conference 2025 (WWW '25), April 28-May 2, 2025, Sydney, NSW, Australia*. ACM, New York, NY, USA, 16 pages. <https://doi.org/10.1145/3696410.3714782>

1 Introduction

Diagnostic errors cause significant harm to healthcare systems worldwide. In the United States, approximately 795,000 individuals each year suffer permanent disability or death due to misdiagnosis of dangerous diseases. These errors are predominantly attributed to cognitive biases and judgmental mistakes [10, 38, 60]. “Healthcare Copilot” is a medical AI assistant designed to provide diagnostic decision support, mitigating biases and increasing efficiency for healthcare practitioners, while also empowering patients and improving overall decision-making [1, 2, 29, 46, 47]. We conducted interviews to gather requirements and suggestions from users of the healthcare copilot. The results showed that one of the most important and challenging tasks for a healthcare copilot is to provide an accurate diagnosis based on patient manifestations¹, followed by offering appropriate treatment plans and medication recommendations based on the diagnosis. In addition, when patient information is insufficient or the diagnosis is ambiguous, the healthcare copilot should proactively offer precise follow-up questions to enhance the decision-making process [3, 26, 40, 47, 68].

Retrieval-augmented generation (RAG) offers an advanced approach by utilizing domain-specific, private datasets to address user queries without the need for additional model training [13, 18, 30]. This approach is well-suited for retrieving information from privacy-sensitive Electronic Health Records (EHRs), and helps healthcare professionals to reduce the risk of misdiagnosis as a healthcare copilot [23, 62]. The existing medical RAG and LLMs

¹“Manifestations” typically include all observable signs and symptoms of a patient’s condition, such as physical indicators (e.g., rash, fever), patient-reported symptoms (e.g., pain, dizziness), and measurable clinical data (e.g., blood pressure, lab results).

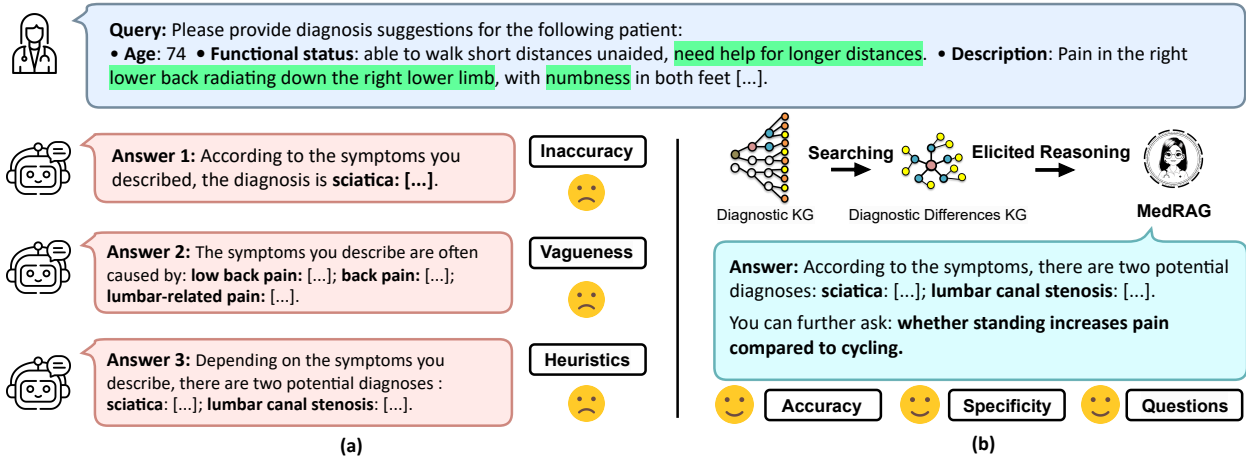


Figure 1: (a) The existing RAG and LLMs rely on heuristic-based approaches, leading to incorrect or vague outputs, particularly when diseases share similar manifestations (high lighted by green colour). (b) MedRAG is a RAG framework with KG-elicted reasoning ability that can make accurate diagnostic decisions and generate highly specific diagnoses, along with proactively providing follow-up questions when necessary.

fine-tuned on medical datasets often rely on heuristic-based approaches, leading to incorrect or vague outputs, particularly when diseases share similar manifestations, making differentiation difficult [19, 25, 32, 61, 65, 69] as shown in Figure 1(a). To address this, we introduce MedRAG, a framework that combines RAG with a comprehensive diagnostic knowledge graph, enabling more accurate reasoning and tailored treatment recommendations by grounding predictions in structured, inferable medical data [22, 27, 36, 56]. This approach significantly enhances the reasoning ability of RAG, enabling it not only to identify subtle diagnostic differences but also to proactively infer relevant follow-up questions, further clarifying ambiguous patient information, as shown in Figure 1(b).

Specifically, a diagnostic knowledge graph (KG) with a four-tier hierarchical structure is constructed systematically through advanced techniques, including disease clustering, hierarchical aggregation and large language model augmentation. While medical ontologies like UMLS could be considered, their ambiguous class definitions and low granularity make them less suitable for direct use. To address these limitations, we construct this KG tailored to each database to eliminate redundancies and enhance manifestations for improved granularity. The diagnostic differences KG searching module then identifies all critical diagnostic differences KG related to the input patient by performing multi-level manifestations matching within the diagnostic KG. Finally, a KG-augmented RAG module synthesizes the retrieved EHRs and the critical diagnostic differences KG to elicit the reasoning within a large language model. This integration enhances the system's ability to make precise and highly specific diagnostic decisions, while also providing personalized treatment recommendations, medication guidance, and, when necessary, proactive follow-up questions.

We evaluate the general applicability of MedRAG by a public dataset DDXPlus [15] and real-world clinical applicability by a private chronic pain diagnostic dataset (CPDD). Performance is quantitatively compared against several popular state-of-the-art (SOTA)

RAG models, including FL-RAG [45] and DRAGIN [52]. We further validate the generalization of MedRAG on widely-used open-source LLMs, including Mixtral-8x7B [21] and Llama-3.1-Instruct [12], as well as on some closed-source LLMs such as GPT-3.5-turbo [41], GPT-4o [42]. Experimental results demonstrate that our model outperforms existing RAG approaches in terms of diagnostic accuracy and specificity. Additionally, MedRAG demonstrates robust generalization across various LLMs, and proves highly effective in generating reasoning-based follow-up diagnostic questions. These capabilities are particularly valuable for distinguishing between diseases with similar manifestations. Based on extensive experiments, our key contributions can be summarized as follows:

- We deliver two diagnostic knowledge graphs: one focused on chronic pain and the other based on DDXPlus [15], a large-scale synthesized dataset. These knowledge graphs contain a rich hierarchical structure of diseases, along with their key diagnostic differences. This comprehensive organization allows for enhanced precision in disease differentiation and diagnosis, enabling better decision-making support across various medical systems.
- We proposed a novel RAG approach enhanced by KG-elicted reasoning, which significantly improves RAG's ability to make accurate and highly specific diagnostic decisions. In addition to supporting personalized treatment recommendations and medication guidance, it proactively generates follow-up questions when necessary. These enhancements greatly optimize the decision-making process in complex medical scenarios.
- Comprehensive experiments conducted on two datasets demonstrate the superiority of our model over existing RAG and LLM approaches. Additionally, the results highlight its applicability across various backbone LLMs and its effectiveness in proactively generating reasoning-based diagnostic questions for medical consultation.

2 Related Works

2.1 LLMs and RAG in Healthcare

Large Language Models (LLMs) have been increasingly applied to healthcare tasks such as EHR analysis, clinical note generation, virtual medical assistant, and clinical decision support [19, 23, 58, 65, 71]. Although LLMs fine-tuned on medical datasets can handle large amounts of unstructured clinical information, most of these models are heuristic-based, with limitations such as generating incorrect or vague information and struggling to handle complex patient cases [25, 65]. To address this, integrating external information sources becomes essential to improve their contextual accuracy. We adopt a Retrieval-Augmented Generation (RAG) approach [30]. RAG enhances LLMs by incorporating retrieved text passages from external sources such as electronic health records, medical papers, textbooks, and databases into their input, resulting in significant improvements in knowledge-intensive tasks [4]. In the field of healthcare, integrating retrieved information grounds the predictions in current, verifiable medical data, resulting in more accurate, specificity and context-aware outputs such as diagnostic assessments and treatment recommendations. RAG typically employs a retrieve-and-read approach to retrieve information based on the initial user query and an answer is generated using that content [14, 17, 28, 49, 51, 73]. However, this simplicity restricts their ability to adapt to complex and evolving medical cases. Enhanced RAG models aim to improve retrieval and generation quality by integrating more sophisticated components such as retrievers, re-rankers, filters, and readers [8, 24, 30, 37, 48, 66]. Despite these advancements, delivering accurate clinical decision support remains challenging. The models often struggle to provide precise diagnoses, particularly when diseases share similar manifestations, making differentiation difficult. Our proposed MedRAG addresses these challenges by systematically constructing a four-tier hierarchical diagnostic knowledge graph to elicit reasoning for the generation module of RAG. This approach enables the model to make accurate diagnostic decisions and generate highly specific diagnoses along with personalized treatment recommendations.

2.2 Knowledge Graph-enhanced LLMs and RAG

Recent studies have focused on creating strategies that integrate knowledge graphs to enhance LLMs and RAG, enabling them to generate accurate and reliable medical responses. Compared to knowledge contained in document repositories [20], knowledge graphs offer structured and inferable information, making them more suitable for augmenting LLMs and RAG [22, 27, 31, 36, 56, 67, 77]. Several works [22, 35, 55, 63, 70, 78] propose training sequence-to-sequence models from scratch, focusing on dialogue generation by conditioning the output on entities extracted from knowledge graphs. However, existing medical knowledge graphs [6, 16, 56, 75] often fall short because they lack the detailed and structured information necessary for accurate diagnostic assistance, especially when distinguishing between diseases with similar manifestations. To overcome this limitation, we introduce MedRAG, a framework that combines RAG with a comprehensive diagnostic knowledge graph to enhance the reasoning ability of RAG in identifying subtle differences in diagnoses. MedRAG allows physicians to input patients' medical records or manifestations. Our knowledge graph

is constructed based on patterns extracted from Electronic Health Record (EHR) databases and augmented by LLMs, making it highly scalable and adaptable to various medical specialties. It supports customization with local databases, ensuring relevance to specific clinical settings. We employ LLMs to enrich the knowledge graph by providing detailed descriptions of the manifestations of each disease at the leaf nodes, including symptoms, affected areas, activity limitations, and other pertinent features.

3 Preliminaries

Definition 3.1 (Diagnostic Knowledge Graph). Given an EHR database D and an LLM \mathcal{M}_a , our target is to construct a four-tier hierarchical diagnostic knowledge graph \mathcal{G} . A multi-hop path, from the top level to the bottom level of \mathcal{G} is represented as $(E_{L1} \xleftarrow{r_s} E_{L2} \xleftarrow{r_s} E_{L3} \xrightarrow{r_m} E_{L4})$. E_{L3} is the set of all diseases (i.e. potential diagnoses) names extracted from D , E_{L2} represents the set of sub-categories of E_{L3} , and E_{L1} is the set of broader categories of E_{L2} . Each e_{Lij} is a disease name or a category name and $e_{Lij} \in E_{Li}$. E_{L1} and E_{L2} are generated by hierarchical aggregation in Section 4.1.1, they indicate the diseases with similar manifestations. r_s is an “is_a” relation, indicating a hierarchical or subordinate relationship. r_m is a “has_manifestation_of” relation between diseases and their manifestations. E_{L4} contains two subtypes: E_{L4a} , representing disease-specific features augmented by the LLM \mathcal{M}_a , and E_{L4d} , representing features decomposed from the manifestations extracted from the EHR database D .

Definition 3.2 (Diagnostic Differences KG Searching). Given a \mathcal{G} and the input patient's manifestations q , let $e_{L2s} \in E_{L2}$ denote a certain subcategory identified through the method described in Section 4.2.3 determined from q . The target is to extract the diagnostic differences KG K , related to e_{L2s} , from \mathcal{G} .

Definition 3.3 (RAG). We define a typical retrieval-augmented generation approach for generating diagnostic reports in two phases: algorithm \mathcal{R} for the retrieval phase and LLM \mathcal{M}_g for the generative phase. A prompt p_{naive} is used to guide \mathcal{M}_g to generate the final report. Given a q , D and embedding model \mathcal{E} , \mathcal{R} retrieves top- k relevant documents d_r , and then \mathcal{M}_g generates answer A with q , d_r and prompt p_{naive} as shown in Equation 1 and 2:

$$d_r = \mathcal{R}(q, D, \mathcal{E}), \quad (1)$$

$$A = \mathcal{M}_g(q, d_r, p_{naive}). \quad (2)$$

4 Methods

In this section, we elaborate on the details of our proposed MedRAG, and the overall framework is illustrated in Figure 2. MedRAG includes five modules:

- **Input:** The input to MedRAG is the description of patient manifestations, which can be either structured EHR or unstructured text descriptions.
- **Output:** The output of MedRAG includes the diagnoses, treatment recommendations, medication guidance and follow-up questions when necessary.
- **Diagnostic Knowledge Graph Construction:** This module constructs a four-tier hierarchical diagnostic knowledge

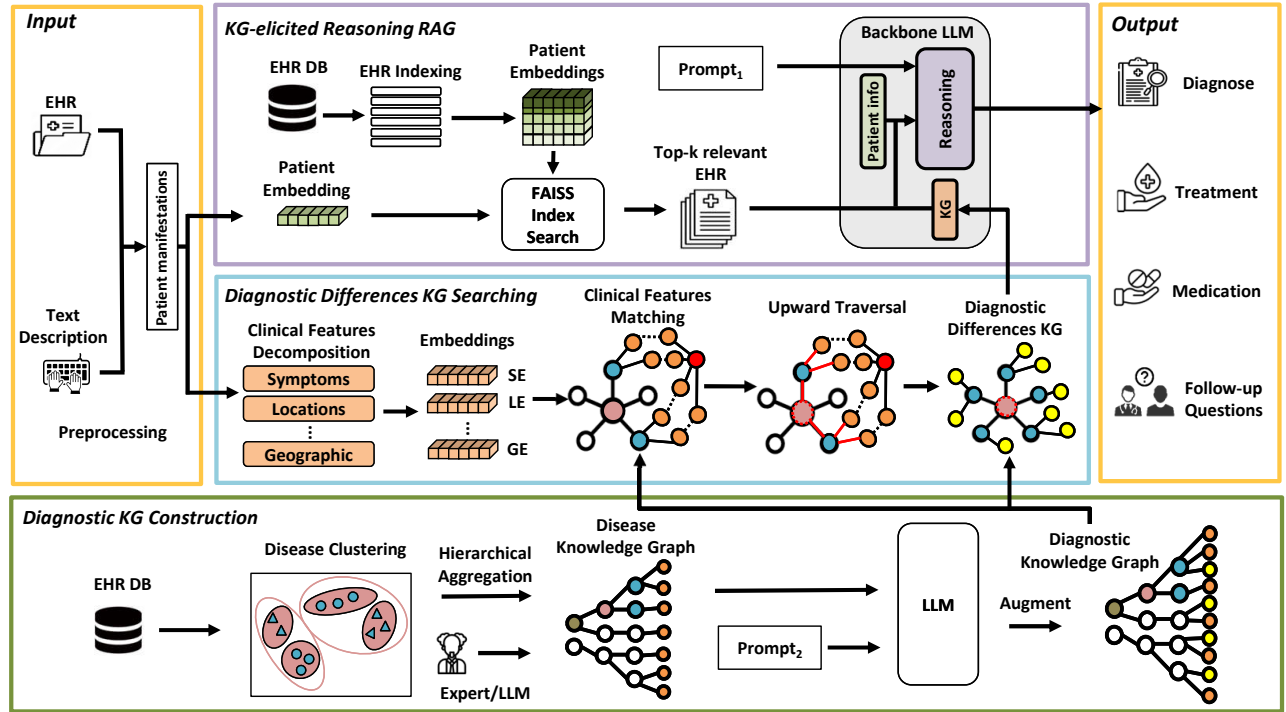


Figure 2: The overall framework of MedRAG. MedRAG first extracts patient (red node) manifestations from structured or unstructured input, and decomposes different clinical features. These features are embedded and matched with a diagnostic KG to identify critical diagnostic differences KG. MedRAG’s KG-elicted reasoning RAG module retrieves relevant EHRs and integrates them with these diagnostic differences KG to trigger reasoning in an LLM. This reasoning generates precise diagnoses, treatment recommendations, and follow-up questions.

graph systematically. First, potential diagnoses and corresponding manifestations are extracted from an EHR database to form a four-tier disease KG through clustering and hierarchical aggregation. Then, an LLM is used to augment the graph with critical diagnostic differences, transforming it into a diagnostic KG.

- **Diagnostic Differences KG Searching:** This module identifies key diagnostic differences by decomposing patient manifestations into clinical features, such as symptoms and locations, through medical chunking. Then, the extracted features are embedded and matched with relevant diagnostic differences via multi-level matching and upward traversal within the diagnostic KG.
- **KG-elicted Reasoning RAG:** This module comprises a document retriever and a KG-elicted reasoning LLM engine. The retriever selects relevant top-k EHRs based on patient embeddings and integrates them with critical diagnostic differences KG to trigger reasoning in the LLM, generating final diagnoses, treatment and medical recommendations and follow-up questions for medical consultation.

4.1 Diagnostic Knowledge Graph Construction

To enhance the reasoning capabilities and fill the knowledge gaps of the RAG, we propose constructing a diagnostic knowledge graph

\mathcal{G} tailored to the medical domain of a specific EHR database. The construction of the diagnostic knowledge graph draws inspiration from the hierarchical structure of the World Health Organization’s International Classification of Diseases, 11th Edition (ICD-11) [43]².

4.1.1 Disease Knowledge Graph Construction. The forms and representations of the diseases in an EHR database are diverse, we first unify the set of original disease descriptions $E_{L3_{raw}}$ by disease clustering to E_{L3} . The most common disease name within each cluster is regarded as the final disease name and is assigned to all other diseases in the cluster, as shown in Equation 3:

$$E_{L3} = C(E_{L3_{raw}}, \mathcal{E}), \quad (3)$$

where C represents the clustering model applied to E_{L3} , \mathcal{E} is an embedding model.

Then we use the unified E_{L3} to construct a four-tier hierarchical disease knowledge graph through hierarchical aggregation. This graph integrates the relationships between diseases and their potential categories, with each disease aggregated into a subcategory and category [74, 76]. We define the disease knowledge graph as

²The specific classification principles of our diagnostic KG and ICD-11 are different. Our approach classifies and organizes diseases based on the similarity of their manifestations, rather than the traditional classification of ICD-11 based on diagnostic categories. As a result, while the hierarchical concept is similar, the ICD-11 structure cannot be directly applied to our model.

\mathcal{G}_D where $\mathcal{G}_D \subset \mathcal{G}$ aggregated by Θ and LLM \mathcal{M}_h , as shown in Equation 4:

$$\mathcal{G}_D = \Theta(E_{L_i}, \mathcal{M}_h, \mathcal{E}), i = 3, 2. \quad (4)$$

In the first phase, we apply LLM-based topic aggregation using \mathcal{M}_h , which extracts the most relevant topics from E_{L3} to aggregate subcategories. These subcategory topics are then further aggregated into higher-level categories, forming the hierarchical structure from subcategories to broader categories. Next, hierarchical clustering is applied to assign diseases in E_{L3} into aggregated subcategory topics and then subtopics to topics.

This approach leverages LLM's powerful semantic understanding and topic extraction capability, allowing for a more nuanced categorization of diseases in topic aggregation. By applying hierarchical clustering to the LLM-based topics, diseases in E_{L3} are aggregated into a hierarchical structure. Hierarchical aggregation introduces multiple layers of granularity to E_{L3} , ensuring that diseases with different manifestations are properly categorized.

To effectively utilize historical diagnoses from D as accurate representations of disease manifestations, we decompose their manifestations of the diseases in E_{L3} , parsing them into discrete features E_{L4d} . Every single feature like symptom, location, or activity limitation from each e_{L3_i} is created as a node $e_{L4d_i} \in E_{L4}$. This final decomposition results in the comprehensive disease knowledge graph \mathcal{G}_D , capturing both disease category information derived from hierarchical aggregation and their associated features.

4.1.2 Knowledge Graph Manifestation Augmentation. The knowledge in \mathcal{G}_D only contains information from D , which is insufficient to accurately diagnose all diseases, particularly when distinguishing between diseases with similar clinical manifestations. Therefore, the integration of external knowledge is essential. To complement the diagnostic knowledge graph with essential knowledge that is not present in D , we augment external knowledge E_{L4} to \mathcal{G}_D that aids in distinguishing diseases with similar manifestations. We traverse all disease e_{L3_i} and employ a prompt p_a specially tailored for searching and generating the nuances of the diseases on an LLM denoted by \mathcal{M}_a . As shown in Equation 5, each generated diagnostic key difference node $e_{L4a_{ij}}$ is then connected to its corresponding e_{L3_i} with relationship r_m . Thus we obtain a chain $E_{L3} \xrightarrow{r_m} E_{L4a}$. For example, we generate a manifestation and relation to disease node *lumbarspondylosis* and form a chain: <*lumbar_spondylosis, has_symptom, stiffness_or_pain_in_the_lower_back*>.

$$\{e_{L3_i}\}_{i=1}^n \xrightarrow{\mathcal{M}_a(p_a, e_{L3_i})} \{e_{L4a_{ij}}\}_{i=1, j=1}^{n, m_i}, \quad (5)$$

$$E_{L4} = E_{L4d} \cup E_{L4a}, \quad (6)$$

$$\mathcal{G} = \mathcal{G}_D \cup_{E_{L3}} \{E_{L3} \cup E_{L4}\}_{i=1}^n, \quad (7)$$

where \mathcal{M}_a and p_a represent the large language model for disease manifestation augmentation and its prompt respectively.

The finalized four-tier hierarchical diagnostic knowledge graph \mathcal{G} is formed by integrating the disease knowledge graph \mathcal{G}_D with E_{L4} combined with E_{L4a} and E_{L4d} , as shown in Equation 6 and 7.

4.2 Diagnostic Differences KG Searching

4.2.1 Decomposition of Manifestations. Given q as a query, which is a description of the patient's manifestations, we perform sentence

trunking on q to decompose the manifestation into more detailed features, denoted as $f_1, f_2, \dots, f_n \in q$. We define a mapping function to describe the process, shown in Equation 8:

$$q \xrightarrow{\phi} \{f_1, f_2, \dots, f_n\}. \quad (8)$$

4.2.2 Clinical Features Matching. Given a q , we compute the semantic similarity score sim between f_i and e_{L4d_j} , shown in Equation 9:

$$sim_{ij} = \mathcal{S}(f_i, e_{L4d_j}, \mathcal{E}), \quad (9)$$

where \mathcal{S} is similarity model and \mathcal{E} is embedding model applied to f_i and e_{L4d_j} before similarity calculation.

For each patient feature f_i , we retrieve the top- m most similar e_{L4d_j} , where m denotes the number of closest matches selected. Totally, the system retrieves $n \times m$ matching nodes in the \mathcal{G} . To address the scenario where a f_i has no closely matching counterpart in E_{L4d} , we introduce an indicator function $\delta(sim_{ij}, t_{matching})$ to filter irrelevant matches:

$$\delta(sim_{ij}, t_{matching}) = \begin{cases} sim_{ij} & \text{if } sim_{ij} > t_{matching} \\ 0 & \text{otherwise,} \end{cases} \quad (10)$$

$$T = \bigcup_{i=1}^n \left\{ e_{L4d_j} \mid j \in \arg \max_{j' \in \{1, \dots, |E_{L4d}| \}} \delta(sim_{ij}, t_{matching}) \right\} \quad (11)$$

where T represents the set of nodes e_{L4d_j} that satisfy the condition $sim_{ij} > t_{matching}$. The indicator function δ ensures that only e_{L4d_j} with a similarity score above the threshold are selected into T . Through clinical features matching, we successfully matched q to the most relevant clinical feature nodes in \mathcal{G} .

4.2.3 Upward Traversal. To precisely match the patient's most relevant e_{L2_s} , we employ upward traversal which determines the closest disease subcategory by aggregating votes based on the shortest path distances between $t_i \in T$ and e_{L2j} in the graph.

For t_i , we calculate the shortest path to each disease subcategory e_{L2j} by upward traversing through the graph. Denote the shortest path distance between t_i to e_{L2j} as $P(t_i, e_{L2j})$. If e_{L2ik} represents the closest disease subcategory node for the current t_i , the vote count for e_{L2ik} is incremented by one. We then accumulate the votes for each e_{L2ik} during the reversal and identify the node with the highest vote count as the e_{L2_s} . This voting process is formalized through the indicator function χ , defined as follows:

$$\chi(t_i, e_{L2ik}) = \begin{cases} 1 & \text{if } e_{L2ik} = \arg \min_{e_{L2j}} P(t_i, e_{L2j}), \\ 0 & \text{otherwise} \end{cases} \quad (12)$$

$$e_{L2_s} = \arg \max_{e_{L2ik}} \sum_{t_i \in T} \chi(t_i, e_{L2ik}), \quad (13)$$

Taking this e_{L2_s} as the parent node, we traverse downward towards E_{L4} , retrieving all e_{L3_i} that are adjacent to e_{L2_s} and their adjacent e_{L4a_j} . Given e_{L2_s} , let $E_{L3_s} = \{e_{L3_i} \mid e_{L3_i} \in \text{Adj}(e_{L2_s})\}$ denote the set of disease nodes that belong to e_{L2_s} . Similarly, define $E_{L4a_s} = \{e_{L4a_j} \mid e_{L4a_j} \in \text{Adj}(e_{L3_i}), e_{L3_i} \in E_{L3_s}\}$ to denote the set of feature nodes linked to the disease nodes in E_{L3_s} .

We concatenate all triples $(e_{L3_s}, r_m, e_{L4a_i})$, where $e_{L3_s} \in \text{Adj}(e_{L2_s})$ and $e_{L4a_i} \in \text{Adj}(e_{L3_s})$, to form the set of diagnostic differences KG:

$$K(e_{L2_s}) = \bigcup_{e_{L3_s} \in \text{Adj}(e_{L2_s})} \{(e_{L3_s}, r_m, e_{L4a_s})\}, \quad (14)$$

where K represents the diagnostic differences KG used for the reasoning in the LLM next.

4.2.4 Proactive Diagnostic Questioning Mechanism. Inaccurate diagnoses often stem from insufficient or incomplete patient descriptions. To address this issue, we propose a Proactive Diagnostic Questioning Mechanism. When the initial input q lacks some crucial information required for doctors or LLMs to make more precise diagnostic decisions, this mechanism acts as a copilot to cast targeted follow-up questions.

In the diagnostic knowledge graph \mathcal{G} , a feature e_{L4d_i} may be connected to multiple disease nodes e_{L3} , with each e_{L4d_i} varying in its discriminability. For instance, certain features are more prevalent, such as “pain located in the lumbar region”, while others represent more distinctive characteristics, like “pain worsens while walking”. Here we define the discriminability score of e_{L4d_i} as the reciprocal of the degree centrality in \mathcal{G} :

$$\sigma(e_{L4d_i}) = \frac{n - 1}{\deg(e_{L4d_i})}, \quad (15)$$

where n represents the total number of e_{L4d_i} .

We calculate the discriminability score $\sigma(e_{L4d_j})$ for each feature node $e_{L4d_j} \in E_{L4d_s}$ and select those with the highest discriminability scores as follows:

$$\{e_{L4d_{s_1}}, e_{L4d_{s_2}}, \dots, e_{L4d_{s_k}}\} = \arg \max_{\{e_{L4d_j} | e_{L4d_j} \in E_{L4d_s}\}} \sigma(e_{L4d_j}), \quad (16)$$

where $\{e_{L4d_{s_1}}, e_{L4d_{s_2}}, \dots, e_{L4d_{s_k}}\}$ represents the selected features with the highest discriminability scores, which are used to proactively guide follow-up questions for clarifying the diagnosis.

4.3 KG-elicited Reasoning RAG

KG-elicited Reasoning RAG is the core component of MedRAG, we use an LLM to generate diagnoses, personalized treatment plans, and medication suggestions. Additionally, the system proactively suggests follow-up questions for doctors to clarify missing or ambiguous patient information. As shown in Equation 17, MedRAG utilizes diagnostic differences KG augmented by LLM and a tailored prompt p_s to elicit the reasoning capabilities of LLM.

$$A = \mathcal{M}_g(q, d_r, K, p_s) \quad (17)$$

Unlike most RAG systems that focus on answering short factual questions, our system is tailored for complex tasks in clinical scenarios. The prompts are designed explicitly to optimize the reasoning capabilities of the LLM, particularly in distinguishing between diseases with similar manifestations. The system conducts thorough reasoning by using both the retrieved documents and the diagnostic differences KG extracted from G .

We use the EHR database as a document repository to retrieve the most relevant documents d_r corresponding to the patient's manifestations q . We then perform a similarity search over the database to identify the most relevant k records. For this, we employ Facebook AI Similarity Search (FAISS) [11], a library optimized for efficient approximate nearest neighbor searches. FAISS allows rapid retrieval of similar records in large-scale EHR datasets, enabling

adjustable trade-offs between speed and search accuracy. After obtaining all inputs, we designed a tailored prompt p_s for guiding the LLM to reason through K , generating answers to assist doctors in distinguishing between similar diseases and proactively generating follow-up questions.

5 Experiments

5.1 Datasets

We evaluate MedRAG using two distinct datasets: one public and one private. The public dataset DDXPlus [15] contains 49 different diagnoses with over 1.3 million patients, each of whom has approximately 10 symptoms and 3 antecedents on average, demonstrating the model's general applicability. The private dataset is the Chronic Pain Diagnostic Dataset (CPDD), a specialized EHR dataset focused on chronic pain patients. This dataset is collected from Tan Tock Seng Hospital, it comprises 551 patients with 33 distinct diagnoses. CPDD offers manifestations-specific chronic pain patient data, making it an invaluable resource for testing MedRAG's diagnostic capabilities in clinical settings. For more details on the public datasets, the partitioning, preprocessing, and experimental setup, please refer to the Appendix.

5.2 Baselines

In order to explore the performance of the MedRAG, we compare the MedRAG results against six other models, including Naive RAG with COT [59], FL-RAG [45], FS-RAG [54], FLARE [25], DRA-GIN [52] and SR-RAG [57]. More detailed introduction to each baseline model is provided in the appendix.

6 Experimental Results

In this section, we present the results of the experiments to answer the following research questions:

- **RQ1:** Does MedRAG outperform the SOTA RAG methods using the same datasets?
- **RQ2:** Does MedRAG demonstrate compatibility, generalizability and adaptability across different backbone LLMs?
- **RQ3:** Does MedRAG's proactive diagnostic questioning mechanism provide users with impactful, relevant follow-up questions to enhance diagnostic performance?
- **RQ4:** Is the MedRAG system we designed effective? What is the impact of each module on its overall performance, and how do specific KG components contribute to MedRAG?

6.1 Quantitative Comparison (RQ1)

Our experiments evaluate MedRAG against six different SOTA RAG models on 2 two datasets. We report the results using: 1) **Accuracy**, defined as the number of correct diagnoses out of the total diagnoses; 2) **Specificity**, which uses $L1$, $L2$, and $L3$ to represent different diagnostic granularity levels. As outlined in Section 3 (Definition 3.1), L_i refers to the MedRAG select potential diagnoses from E_{L_i} . This metric evaluates the model's specificity and its ability to differentiate between similar diseases across varying levels of diagnostic granularity; 3) **Text Generation Metrics**, which uses BERTScore, BLEU, ROUGE, METEOR and subjective evaluation from doctors to evaluate generated reports.

Method	Model	CPDD			DDXPlus		
		L1	L2	L3	L1	L2	L3
Baselines	Naive RAG + COT	75.47	54.72	43.40	79.28	71.89	56.84
	FS-RAG	64.71	49.02	45.10	78.18	68.20	51.40
	FLARE	54.84	48.39	45.16	71.09	56.70	31.02
	FL-RAG	65.45	50.91	49.09	90.12	83.32	<u>66.78</u>
	DRAGIN	78.72	59.57	40.42	80.51	70.83	50.24
	SR-RAG	73.58	<u>60.38</u>	<u>54.72</u>	78.65	70.28	52.16
Ours	MedRAG	79.25	75.47	66.04	88.65	83.46	68.01

Table 1: Results of quantitative performance comparison

	Backbone LLMs	Size	w/o KG-elicited Reasoning			w/ KG-elicited Reasoning		
			L1	L2	L3	L1	L2	L3
Open-source Models	Mixtral-8x7B	13B	60.38	32.08	22.34	84.62	<u>82.69</u>	63.46
	Qwen-2.5	72B	<u>66.04</u>	41.51	39.62	80.36	<u>73.21</u>	64.29
	Llama-3.1-Instruct	8B	75.47	54.72	43.40	79.25	75.47	66.04
	Llama-3.1-Instruct	70B	86.79	<u>67.92</u>	<u>56.60</u>	<u>86.79</u>	83.02	<u>71.70</u>
Closed-source Models	GPT-3.5-turbo	-	83.02	56.60	45.28	70.56	68.68	50.57
	GPT-4o-mini	-	<u>88.68</u>	<u>67.92</u>	<u>56.60</u>	85.85	75.00	60.38
	GPT-4o	-	90.57	71.70	60.38	91.87	81.78	73.23

Table 2: Performance of MedRAG on different LLM backbones with and without KG-elicited reasoning

The disease prediction result is shown in Table 1, MedRAG achieved the best or second-best (with only one exception) performance across multiple metrics in all datasets. Accuracy on the *L3* metric is the best indicator of MedRAG’s performance, as higher specificity increases diagnostic difficulty. MedRAG outperformed the second-best scores on the CPDD and DDXPlus datasets by 11.32% and 1.23%.

Additionally, most RAG models designed for simpler QA tasks do not perform as well in the more complex medical domain, leading to longer contextual and prompt. These models are often optimized for generating short and straightforward answers, which limits their effectiveness in handling intricate medical queries. We observe models that have a simpler mechanism in the query-organizing phase perform better than part of more sophisticated ones. Except for our MedRAG, models like SR-RAG and FL-RAG also secured several second-best performances. Even the Chain-of-Thought model, which lacks improvements in the retriever or generator components, outperformed some of the other SOTA models in complex medical tasks.

For report generation evaluation, we conducted both objective and subjective assessments. The objective evaluation used the standard rule-based text generation metrics: BERTScore [72], BLEU [44], ROUGE [34], METEOR [5]. The subjective evaluation followed Mini-CEX (Clinical Evaluation Exercise) [39], a clinical assessment framework that has been incorporated into LLMs for report evaluation [50]. To ensure reliability, we consulted doctors to review and validate the results. Details are in the Appendix.

6.2 Compatibility, Generalizability and Adaptability (RQ2)

The results in Table 2 demonstrate the performance of incorporating KG-elicited reasoning to various backbone LLMs, including both open-source and closed-source models. The results demonstrate that the inclusion of KG-elicited reasoning significantly enhances diagnostic accuracy across *L1*, *L2*, and *L3* for all backbone LLMs. For example, Mixtral-8x7B shows a significant *L3* improvement from 22.34% to 63.46%, demonstrating the effectiveness of our proposed KG-elicited reasoning, particularly in smaller models.

Among both open-source and closed-source models, the RAG with the GPT-4o as the backbone LLM outperforms all others, showing its superior adaptability with knowledge graph integration. Additionally, MedRAG achieves the best performance on closed-source models, highlighting its compatibility, generalizability, and adaptability. In contrast, token-level RAG models like DRAGIN and FLARE face challenges in adapting to closed-source models due to their inherent frameworks, limiting their potential to achieve better performance across various LLMs.

We also observe an interesting result that incorporating KG into small-scale closed-source models reduces *L1* performance. We deduce that introducing similar disease difference complicates the reasoning. GPT-3.5 and GPT-4o-mini struggle with incorporating highly granular information due to parameter limitations, leading to knowledge conflicts and blurred classification boundaries, which impact *L1* performance. However, GPT-4o’s larger parameter scale and stronger reasoning capacity result in higher *L1* accuracy.

6.3 Proactive Diagnostic Questioning (RQ3)

The results in Table 3 show the impact of following MedRAG's optimized instructive questions and obtaining corresponding patient responses on diagnostic accuracy.

Manifestation Masking Ratio	<i>L1</i>	<i>L2</i>	<i>L3</i>
100%	60.38	56.60	52.83
66.6%	69.39	67.35	55.10
33.3%	71.43	67.35	61.22
0%	79.25	75.47	66.04

Table 3: Result of proactive diagnostic questioning

As more detailed information is gathered through these targeted questions, the *L3* accuracy progressively improves. Initially, with no specific patient information obtained through this questioning process, the *L3* accuracy is 52.83%, representing MedRAG making a diagnosis with other information with very few manifestations. As the doctor collects more critical details about disease representation, covering from 33.3% to 100% of the key manifestations, the *L3* score rises from 55.10% to 66.04% and other levels' metrics follow the same trend. This demonstrates the significant effectiveness of MedRAG's proactive diagnostic questioning mechanism, validating its capability to provide doctors with impactful questions that not only enhance diagnostic performance but also improve the efficiency of the medical consultation process.

6.4 Ablation Study (RQ4)

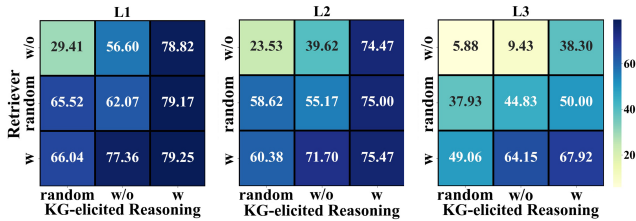


Figure 3: Ablation result on Llama-3.1-Instruct 8B backbone using the CPDD dataset

We perform ablation studies to evaluate the effectiveness of different components in MedRAG and present the result in Figure 3. Specifically, we assess the retriever \mathcal{R} and KG-elicit reasoning module \mathcal{G} under three configurations: "random", "with" and "without". In the "random" setting for \mathcal{R} , we choose documents from the entire EHR database randomly. The "without" of the retriever refers to the scenario where no documents are passed to \mathcal{M}_g . The "with" setting of the retriever means to pass the top- k relevant documents to \mathcal{M}_g . For the KG-elicit reasoning module, the "random" configuration denotes randomly selecting subcategory e_{L2_s} and collecting corresponding K accordingly. The "without" is the scenario where no diagnostic differences KG are passed to \mathcal{M}_g . Configuration "with" means to pass correct K by the e_{L2_s} to \mathcal{M}_g .

As shown in Figure 3, both the retriever and KG-elicit reasoning module significantly enhance performance across all specificity

levels. the best outcomes are achieved when RAG and KG components are combined and aligned, especially for granular diagnosis tasks that demand high specificity. Notably, randomly selected documents performed better than no documents at all, this phenomenon was explored in detail by [9]. We also observed a performance decline in the lower-granularity levels of *L1* and *L2* when transitioning from random to no knowledge from KG when random documents are retrieved. Once correct KG-augmented knowledge was added, this noise effect was mitigated, leading to accuracy improvements across all metrics: an average accuracy increase of 18.88% for *L1*, 26.92% for *L2*, and 18.89% for *L3*, compared to the baseline with random or without KG-elicit reasoning module. The ablation study of KG components is shown in the Appendix.

7 Conclusion

In conclusion, MedRAG significantly improves diagnostic accuracy and specificity in the medical domain by integrating KG-elicit reasoning with RAG models. By systematically retrieving and reasoning over EHRs and dynamically incorporating critical diagnostic differences KG, MedRAG offers more precise diagnosis and personalized treatment recommendations. Additionally, MedRAG's proactive diagnostic questioning mechanism effectively enhances diagnostic performance and consultation efficiency by generating impactful questions for doctors and patients. The evaluation of public and private datasets demonstrates that MedRAG outperforms state-of-the-art RAG models, particularly in reducing misdiagnosis rates for diseases with similar manifestations, showcasing its potential as a key module in healthcare copilot.

For future work, we aim to integrate multimodal data, including imaging, physiological signals, etc., and deploy the MedRAG system in hospitals for real-world testing. Furthermore, to improve usability for doctors, we will integrate a speech recognition module into the system. For further details, please refer to the Appendix.

Acknowledgments

This research is supported by the Joint NTU-UBC Research Centre of Excellence in Active Living for the Elderly (LILY) and the College of Computing and Data Science (CCDS) at NTU Singapore. It is also partially supported by the Singapore Ministry of Education Academic Research Fund Tier 1 (Grant No. 2017-T1-001-270). This research is also supported, in part, by the National Research Foundation, Prime Minister's Office, Singapore under its NRF Investigatorship Programme (NRFI Award No. NRF-NRFI05-2019-0002). Any opinions, findings, conclusions, or recommendations expressed in this material are those of the authors and do not reflect the views of National Research Foundation, Singapore. This research is supported, in part, by the Singapore Ministry of Health under its National Innovation Challenge on Active and Confident Ageing (NIC Project No. MOH/NIC/HAIG03/2017). This research is supported, in part, by the RIE2025 Industry Alignment Fund – Industry Collaboration Projects (IAF-ICP) (Award I2301E0026), administered by A*STAR, as well as partially supported by Alibaba Group and NTU Singapore through Alibaba-NTU Global e-Sustainability CorpLab (ANGEL). This work is partially supported by the Wallenberg AI, Autonomous Systems and Software Program (WASP) funded by the Knut and Alice Wallenberg Foundation.

References

- [1] 2024. Doctor Co-Pilot. <https://demos.amotion.ai/3>. Accessed: 2024-10-11.
- [2] 2024. Microsoft Copilot in Healthcare. <https://www.avanade.com/en/services/artificial-intelligence/ai-copilot-hub/health-ai-copilot>. Accessed: 2024-10-11.
- [3] Durga Prasad Ambala. 2023. AI-Powered Copilot for Healthcare Sales Agents: Enhancing Customer Engagement and Test Recommendations. *Journal of Scientific and Engineering Research* 10, 10 (2023), 164–167.
- [4] Akari Asai, Zeqiu Wu, Yizhong Wang, Avirup Sil, and Hannaneh Hajishirzi. 2023. Self-rag: Learning to retrieve, generate, and critique through self-reflection. *arXiv preprint arXiv:2310.11511* (2023).
- [5] Satanjeev Banerjee and Alon Lavie. 2005. METEOR: An automatic metric for MT evaluation with improved correlation with human judgments. In *Proceedings of the acl workshop on intrinsic and extrinsic evaluation measures for machine translation and/or summarization*. 65–72.
- [6] Payal Chandak, Kexin Huang, and Marinka Zitnik. 2023. Building a knowledge graph to enable precision medicine. *Scientific Data* 10, 1 (2023), 67.
- [7] Siyuan Chen, Mengyue Wu, Kenny Q Zhu, Kunyao Lan, Zhiling Zhang, and Lychun Cui. 2023. LLM-empowered chatbots for psychiatrist and patient simulation: application and evaluation. *arXiv preprint arXiv:2305.13614* (2023).
- [8] Hao Cheng, Yelong Shen, Xiaodong Liu, Pengcheng He, Weizhu Chen, and Jianfeng Gao. 2021. UnitedQA: A hybrid approach for open domain question answering. *arXiv preprint arXiv:2101.00178* (2021).
- [9] Florin Cuconas, Giovanni Trappolini, Federico Siciliano, Simone Filice, Cesare Campagnano, Yoelle Maarek, Nicola Tonello, and Fabrizio Silvestri. 2024. The power of noise: Redefining retrieval for rag systems. In *Proceedings of the 47th International ACM SIGIR Conference on Research and Development in Information Retrieval*. 719–729.
- [10] Ram A Dixit, Christian L Boxley, Sunil Samuel, Vishnu Mohan, Raj M Ratwani, and Jeffrey A Gold. 2023. Electronic health record use issues and diagnostic error: a scoping review and framework. *Journal of patient safety* 19, 1 (2023), e25–e30.
- [11] Matthijs Douze, Alexandre Guzhva, Chengqi Deng, Jeff Johnson, Gergely Szilvassy, Pierre-Emmanuel Mazaré, Maria Lomeli, Lucas Hosseini, and Hervé Jégou. 2024. The faiss library. *arXiv preprint arXiv:2401.08281* (2024).
- [12] Abhimanyu Dubey, Abhinav Jauhri, Abhinav Pandey, Abhishek Kadian, Ahmad Al-Dahle, Aiesha Letman, Akhil Mathur, Alan Schelten, Amy Yang, Angela Fan, et al. 2024. The llama 3 herd of models. *arXiv preprint arXiv:2407.21783* (2024).
- [13] Darren Edge, Ha Trinh, Newman Cheng, Joshua Bradley, Alex Chao, Apurva Mody, Steven Truitt, and Jonathan Larson. 2024. From local to global: A graph rag approach to query-focused summarization. *arXiv preprint arXiv:2404.16130* (2024).
- [14] Wenyi Fan, Yujuan Ding, Liangbo Ning, Shijie Wang, Hengyun Li, Dawei Yin, Tat-Seng Chua, and Qing Li. 2024. A survey on rag meeting llms: Towards retrieval-augmented large language models. In *Proceedings of the 30th ACM SIGKDD Conference on Knowledge Discovery and Data Mining*. 6491–6501.
- [15] Arsene Fansi Tchang, Rishab Goel, Zhi Wen, Julien Martel, and Joumana Ghosn. 2022. Ddxplus: A new dataset for automatic medical diagnosis. *Advances in neural information processing systems* 35 (2022), 31306–31318.
- [16] Yanjun Gao, Ruizhe Li, John Caskey, Dmitriy Dligach, Timothy Miller, Matthew M Churpek, and Majid Afshar. 2023. Leveraging a medical knowledge graph into large language models for diagnosis prediction. *arXiv preprint arXiv:2308.14321* (2023).
- [17] Yifu Gao, Linbo Qiao, Zhigang Kan, Zhihua Wen, Yongquan He, and Dongsheng Li. 2024. Two-stage Generative Question Answering on Temporal Knowledge Graph Using Large Language Models. *arXiv preprint arXiv:2402.16568* (2024).
- [18] Kelvin Guu, Kenton Lee, Zora Tung, Panupong Pasupat, and Mingwei Chang. 2020. Retrieval augmented language model pre-training. In *International conference on machine learning*. PMLR, 3929–3938.
- [19] Tianyu Han, Lisa C Adams, Jens-Michalis Papaioannou, Paul Grundmann, Tom Oberhauser, Alexander Löser, Daniel Truhn, and Keno K Bressem. 2023. MedAlpaca—An Open-Source Collection of Medical Conversational AI Models and Training Data. *arXiv preprint arXiv:2304.08247* (2023).
- [20] Gautier Izacard, Mathilde Caron, Lucas Hosseini, Sebastian Riedel, Piotr Bojanowski, Armand Joulin, and Edouard Grave. 2021. Unsupervised dense information retrieval with contrastive learning. *arXiv preprint arXiv:2112.09118* (2021).
- [21] Albert Q Jiang, Alexandre Sablayrolles, Antoine Roux, Arthur Mensch, Blanche Savary, Chris Bamford, Devendra Singh Chaplot, Diego de las Casas, Emma Bou Hanna, Florian Bressand, et al. 2024. Mixtral of experts. *arXiv preprint arXiv:2401.04088* (2024).
- [22] Jinbiao Jiang, Kun Zhou, Wayne Xin Zhao, Yaliang Li, and Ji-Rong Wen. 2023. Reasoninglm: Enabling structural subgraph reasoning in pre-trained language models for question answering over knowledge graph. *arXiv preprint arXiv:2401.00158* (2023).
- [23] Xinkie Jiang, Yue Fang, Rihong Qiu, Haoyu Zhang, Yongxin Xu, Hao Chen, Wentao Zhang, Ruizhe Zhang, Yuchen Fang, Xu Chu, et al. 2024. TC-RAG: Turing-Complete RAG's Case study on Medical LLM Systems. *arXiv preprint arXiv:2408.09199* (2024).
- [24] Xinkie Jiang, Ruizhe Zhang, Yongxin Xu, Rihong Qiu, Yue Fang, Zhiyuan Wang, Jinyi Tang, Hongxin Ding, Xu Chu, Junfeng Zhao, et al. 2024. HyKGE: A Hypothesis Knowledge Graph Enhanced Framework for Accurate and Reliable Medical LLMs Responses. *arXiv preprint arXiv:2312.15883* (2024).
- [25] Zhengbao Jiang, Frank F Xu, Luyu Gao, Zhiqing Sun, Qian Liu, Jane Dwivedi-Yu, Yiming Yang, Jamie Callan, and Graham Neubig. 2023. Active retrieval augmented generation. *arXiv preprint arXiv:2305.06983* (2023).
- [26] Wall Street Journal. 2023. OpenAI Expands Healthcare Push With Color Health's Cancer Copilot. *The Wall Street Journal* (2023). <https://www.wsj.com/articles/openai-expands-healthcare-push-with-color-healths-cancer-copilot-86594ff1> Accessed: 2024-09-18.
- [27] Minki Kang, Jin Myung Kwak, Jinheon Baek, and Sung Ju Hwang. 2023. Knowledge graph-augmented language models for knowledge-grounded dialogue generation. *arXiv preprint arXiv:2305.18846* (2023).
- [28] Urvashi Khandelwal, Omer Levy, Dan Jurafsky, Luke Zettlemoyer, and Mike Lewis. 2019. Generalization through memorization: Nearest neighbor language models. *arXiv preprint arXiv:1911.00172* (2019).
- [29] Ching Hung Lee, Zehao Zhang, and Xuejiao Zhao. 2021. A survey of smart healthcare for the elderly based on user requirements and supply accessibility. In *5th International Conference on Crowd Science and Engineering*. 108–112.
- [30] Patrick Lewis, Ethan Perez, Aleksandra Piktus, Fabio Petroni, Vladimir Karpukhin, Naman Goyal, Heinrich Küttler, Mike Lewis, Wen-tau Yih, Tim Rocktäschel, et al. 2020. Retrieval-augmented generation for knowledge-intensive nlp tasks. *Advances in Neural Information Processing Systems* 33 (2020), 9459–9474.
- [31] Hongwei Li, Sirui Li, Jiamou Sun, Zhenchang Xing, Xin Peng, Mingwei Liu, and Xuejiao Zhao. 2018. Improving api caveats accessibility by mining api caveats knowledge graph. In *2018 IEEE International Conference on Software Maintenance and Evolution (ICSME)*. IEEE, 183–193.
- [32] Yunxiang Li, Zihan Li, Kai Zhang, Ruilong Dan, Steve Jiang, and You Zhang. 2023. Chatdoctor: A medical chat model fine-tuned on a large language model meta-ai (llama) using medical domain knowledge. *Cureus* 15, 6 (2023).
- [33] Zhiang Li and Tong Ruan. 2024. Knowledge-routed Automatic Diagnosis with Heterogeneous Patient-oriented Graph. *IEEE Access* (2024).
- [34] Chin-Yew Lin. 2004. Rouge: A package for automatic evaluation of summaries. In *Text summarization branches out*. 74–81.
- [35] Ye Liu, Yao Wan, Lifang He, Hao Peng, and S Yu Philip. 2021. Kg-bart: Knowledge graph-augmented bart for generative commonsense reasoning. In *Proceedings of the AAAI conference on artificial intelligence*, Vol. 35. 6418–6425.
- [36] Linhao Luo, Yuan-Fang Li, Gholamreza Haffari, and Shirui Pan. 2023. Reasoning on graphs: Faithful and interpretable large language model reasoning. *arXiv preprint arXiv:2310.01061* (2023).
- [37] Kaixin Ma, Hao Cheng, Yu Zhang, Xiaodong Liu, Eric Nyberg, and Jianfeng Gao. 2023. Chain-of-skills: A configurable model for open-domain question answering. *arXiv preprint arXiv:2305.03130* (2023).
- [38] David E Newman-Toker, Najla Nassery, Adam C Schaffer, Chihwen Winnie Yu-Moe, Gwendolyn D Clemens, Zheyu Wang, Yuxin Zhu, Ali S Saber Tehrani, Mehdi Fanai, Ahmed Hassoon, et al. 2024. Burden of serious harms from diagnostic error in the USA. *BMJ Quality & Safety* 33, 2 (2024), 109–120.
- [39] John J Norcini, Linda L Blank, Gerald K Arnold, and Harry R Kimball. 1995. The mini-CEX (clinical evaluation exercise): a preliminary investigation. *Annals of internal medicine* 123, 10 (1995), 795–799.
- [40] OpenAI. 2023. Color Health's Cancer Copilot. <https://openai.com/index/color-health/> Accessed: 2024-09-18.
- [41] OpenAI. 2024. ChatGPT. <https://openai.com/index/chatgpt/> Accessed: 2024-10-07.
- [42] OpenAI. 2024. GPT-4o. <https://openai.com/index/hello-gpt-4o/> Accessed: 2024-10-07.
- [43] World Health Organization et al. 1992. ICD-11. (*No Title*) (1992).
- [44] Kishore Papineni, Salim Roukos, Todd Ward, and Wei-Jing Zhu. 2002. Bleu: a method for automatic evaluation of machine translation. In *Proceedings of the 40th annual meeting of the Association for Computational Linguistics*. 311–318.
- [45] Ori Ram, Yoav Levine, Itay Dalmedigo, Dor Muhlgray, Amnon Shashua, Kevin Leyton-Brown, and Yoav Shoham. 2023. In-context retrieval-augmented language models. *Transactions of the Association for Computational Linguistics* 11 (2023), 1316–1331.
- [46] Haocong Rao, Minlin Zeng, Xuejiao Zhao, and Chunyan Miao. 2024. A Survey of Artificial Intelligence in Gait-Based Neurodegenerative Disease Diagnosis. *arXiv preprint arXiv:2405.13082* (2024).
- [47] Zhiyao Ren, Yibing Zhan, Baosheng Yu, Liang Ding, and Dacheng Tao. 2024. Healthcare copilot: Eliciting the power of general llms for medical consultation. *arXiv preprint arXiv:2402.13408* (2024).
- [48] Parth Sarthi, Salman Abdullah, Aditi Tuli, Shubh Khanna, Anna Goldie, and Christopher D Manning. 2024. Raptor: Recursive abstractive processing for tree-organized retrieval. *arXiv preprint arXiv:2401.18059* (2024).
- [49] Priyanka Sen, Sandeep Mavadia, and Amir Saffari. 2023. Knowledge graph-augmented language models for complex question answering. In *Proceedings of the 1st Workshop on Natural Language Reasoning and Structured Explanations (NLRSE)*. 1–8.

- [50] Xiaoming Shi, Jie Xu, Jinru Ding, Jiali Pang, Sichen Liu, Shuqing Luo, Xingwei Peng, Lu Lu, Haihong Yang, Mingtao Hu, et al. 2023. Llm-mini-cex: Automatic evaluation of large language model for diagnostic conversation. *arXiv preprint arXiv:2308.07635* (2023).
- [51] Karthik Soman, Peter W Rose, John H Morris, Rabia E Akbas, Brett Smith, Braian Peetoom, Catalina Villouta-Reyes, Gabriel Ceroni, Yongmei Shi, Angela Rizk-Jackson, et al. 2023. Biomedical knowledge graph-enhanced prompt generation for large language models. *arXiv preprint arXiv:2311.17330* (2023).
- [52] Weihang Su, Yichen Tang, Qingyao Ai, Zhijing Wu, and Yiqun Liu. 2024. Dragin: Dynamic retrieval augmented generation based on the real-time information needs of large language models. *arXiv preprint arXiv:2403.10081* (2024).
- [53] Zhi Rui Tam, Cheng-Kuang Wu, Yi-Lin Tsai, Chieh-Yen Lin, Hung-yi Lee, and Yun-Nung Chen. 2024. Let me speak freely? a study on the impact of format restrictions on performance of large language models. *arXiv preprint arXiv:2408.02442* (2024).
- [54] Harsh Trivedi, Nirjanan Balasubramanian, Tushar Khot, and Ashish Sabharwal. 2022. Interleaving retrieval with chain-of-thought reasoning for knowledge-intensive multi-step questions. *arXiv preprint arXiv:2212.10509* (2022).
- [55] Yi-Lin Tuan, Yun-Nung Chen, and Hung-yi Lee. 2019. Dykgchat: Benchmarking dialogue generation grounding on dynamic knowledge graphs. *arXiv preprint arXiv:1910.00610* (2019).
- [56] Deeksha Varshney, Aizan Zafar, Niranshu Kumar Behera, and Asif Ekbal. 2023. Knowledge graph assisted end-to-end medical dialog generation. *Artificial Intelligence in Medicine* 139 (2023), 102535.
- [57] Jing Wang, Zien Cheng, Qiuming Yao, Li Liu, Dong Xu, and Gangqing Hu. 2024. Bioinformatics and biomedical informatics with ChatGPT: Year one review. *Quantitative Biology* (2024).
- [58] Zixiang Wang, Yinghai Zhu, Junyi Gao, Xiaochen Zheng, Yuhui Zeng, Yifan He, Bowen Jiang, Wen Tang, Ewen M Harrison, Chengwei Pan, et al. [n. d.]. RetCare: Towards Interpretable Clinical Decision Making through LLM-Driven Medical Knowledge Retrieval. In *Artificial Intelligence and Data Science for Healthcare: Bridging Data-Centric AI and People-Centric Healthcare*.
- [59] Jason Wei, Xuezhi Wang, Dale Schuurmans, Maarten Bosma, Fei Xia, Ed Chi, Quoc V Le, Denny Zhou, et al. 2022. Chain-of-thought prompting elicits reasoning in large language models. *Advances in neural information processing systems* 35 (2022), 24824–24837.
- [60] Sidong Wei, Xuejiao Zhao, and Chunyan Miao. 2018. A comprehensive exploration to the machine learning techniques for diabetes identification. In *2018 IEEE 4th World Forum on Internet of Things (WF-IoT)*. IEEE, 291–295.
- [61] Chaoyi Wu, Weixiong Lin, Xiaoman Zhang, Ya Zhang, Weidi Xie, and Yanfeng Wang. 2024. PMC-LLaMA: toward building open-source language models for medicine. *Journal of the American Medical Informatics Association* (2024), ocaec045.
- [62] Junde Wu, Jiayuan Zhu, and Yunli Qi. 2024. Medical Graph RAG: Towards Safe Medical Large Language Model via Graph Retrieval-Augmented Generation. *arXiv preprint arXiv:2408.04187* (2024).
- [63] Sixing Wu, Ying Li, Dawei Zhang, Yang Zhou, and Zhonghai Wu. 2020. Diverse and informative dialogue generation with context-specific commonsense knowledge awareness. In *Proceedings of the 58th annual meeting of the association for computational linguistics*. 5811–5820.
- [64] Yunfei Xie, Juncheng Wu, Haoqin Tu, Siwei Yang, Bingchen Zhao, Yongshuo Zong, Qiao Jin, Cihang Xie, and Yuyin Zhou. 2024. A Preliminary Study of o1 in Medicine: Are We Closer to an AI Doctor? *arXiv preprint arXiv:2409.15277* (2024).
- [65] Ziqi Yang, Xuhai Xu, Bingsheng Yao, Ethan Rogers, Shao Zhang, Stephen Intille, Nawar Shara, Guodong Gordon Gao, and Dakuo Wang. 2024. Talk2Care: An LLM-based Voice Assistant for Communication between Healthcare Providers and Older Adults. *Proceedings of the ACM on Interactive, Mobile, Wearable and Ubiquitous Technologies* 8, 2 (2024), 1–35.
- [66] Ori Yoran, Tomer Wolfson, Ori Ram, and Jonathan Berant. 2023. Making retrieval-augmented language models robust to irrelevant context. *arXiv preprint arXiv:2310.01558* (2023).
- [67] Donghan Yu, Chengguang Zhu, Yuwei Fang, Wenhao Yu, Shuhang Wang, Yichong Xu, Xiang Ren, Yiming Yang, and Michael Zeng. 2021. Kg-fid: Infusing knowledge graph in fusion-in-decoder for open-domain question answering. *arXiv preprint arXiv:2110.04330* (2021).
- [68] Cyril Zakka, Joseph Cho, Gracia Fahed, Rohan Shad, Michael Moor, Robyn Fong, Dhamanpreet Kaur, Vishnu Rav, Oliver Aalami, Roxana Daneshjou, et al. 2024. Almanac Copilot: Towards Autonomous Electronic Health Record Navigation. *arXiv preprint arXiv:2405.07896* (2024).
- [69] Charlotte Zelin, Wendy K Chung, Mederic Jeanne, Gongbo Zhang, and Chunhua Weng. 2024. Rare disease diagnosis using knowledge guided retrieval augmentation for ChatGPT. *Journal of Biomedical Informatics* 157 (2024), 104702.
- [70] Houyu Zhang, Zhenghao Liu, Chenyan Xiong, and Zhiyuan Liu. 2019. Grounded conversation generation as guided traverses in commonsense knowledge graphs. *arXiv preprint arXiv:1911.02707* (2019).
- [71] Kai Zhang, Yangyang Kang, Fubang Zhao, and Xiaozhong Liu. 2024. LLM-based Medical Assistant Personalization with Short-and Long-Term Memory Coordination. In *Proceedings of the 2024 Conference of the North American Chapter of the Association for Computational Linguistics: Human Language Technologies (Volume 1: Long Papers)*. 2386–2398.
- [72] Tianyi Zhang, Varsha Kishore, Felix Wu, Kilian Q Weinberger, and Yoav Artzi. 2019. Bertscore: Evaluating text generation with bert. *arXiv preprint arXiv:1904.09675* (2019).
- [73] Penghao Zhao, Hailin Zhang, Qinhan Yu, Zhengren Wang, Yunteng Geng, Fangcheng Fu, Ling Yang, Wentao Zhang, and Bin Cui. 2024. Retrieval-augmented generation for ai-generated content: A survey. *arXiv preprint arXiv:2402.19473* (2024).
- [74] Xuejiao Zhao. 2021. Explainable Q&A system based on domain-specific knowledge graph. (2021).
- [75] Xuejiao Zhao, Huanhuan Chen, Zhenchang Xing, and Chunyan Miao. 2021. Brain-inspired search engine assistant based on knowledge graph. *IEEE Transactions on Neural Networks and Learning Systems* 34, 8 (2021), 4386–4400.
- [76] Xuejiao Zhao, Zhenchang Xing, Muhammad Ashad Kabir, Naoya Sawada, Jing Li, and Shang-Wei Lin. 2017. Hdskg: Harvesting domain specific knowledge graph from content of webpages. In *2017 ieee 24th international conference on software analysis, evolution and reengineering (saner)*. IEEE, 56–67.
- [77] Lingfeng Zhong, Jia Wu, Qian Li, Hao Peng, and Xindong Wu. 2023. A comprehensive survey on automatic knowledge graph construction. *Comput. Surveys* 56, 4 (2023), 1–62.
- [78] Hao Zhou, Minlie Huang, Yong Liu, Wei Chen, and Xiaoyan Zhu. 2021. EARL: informative knowledge-grounded conversation generation with entity-agnostic representation learning. In *Proceedings of the 2021 Conference on Empirical Methods in Natural Language Processing*. 2383–2395.

Appendix

This appendix is organized as follows:

- **Section A** includes variables and definitions in the paper.
- **Section B** demonstrates the detailed data preprocessing steps and experimental setup, ensuring transparency and reproducibility.
- **Section C** describes the details of the baseline models in the experiments.
- **Section D** presents intermediate results from experiments.
- **Section E** shows the evaluation of report generation.
- **Section F** shows the ablation study on KG components.
- **Section G** shows the user interface of the healthcare copilot.
- **Section H** show the future work of this paper.

A Variables and Definitions

The variables used throughout this paper and their definitions are provided in Table A3.

B Data Preprocessing and Experimental Setup

B.1 Datasets

The public dataset, DDXPlus [15], is a large-scale synthesized EHR dataset, recognized for its complex and diverse medical cases. It includes comprehensive patient data such as socio-demographic information, underlying diseases, symptoms, and antecedents, addressing the symptom-related data gap in common EHR datasets like MIMIC [15]. Many studies have employed DDXPlus to benchmark models in medical reasoning and diagnosis [7, 33, 53, 64]. DDXPlus contains 49 different diagnoses with over 1.3 million patients, each of whom has approximately 10 symptoms and 3 antecedents on average. We ultimately utilized a maximum balanced sub-dataset comprising 13,230 patients' EHRs.

B.2 Settings for Datasets

- **CPDD** We split the data set into a 9:1 ratio for the training set (to be retrieved) and test set. Since the dataset was collected from multiple doctors, the diagnosis descriptions are not standardized. Part of the diagnosis is presented as a type of pain instead of a specific disease. When calculating the accuracy of these pain-type diagnoses, if the predicted result is a disease associated with that type of pain, it will be considered a correct prediction.
- **DDXPlus** We directly use the training set and test set in a split dataset in the ratio of 8:1:1(validation set). Due to the massive size of the dataset with over a million synthesized patients' records, which is too large for the scale of our task, we first fixed the number of samples in the test set to 30, which corresponds to the fewest pathology. For the other pathology with more samples, we randomly select 30 samples to form the whole test set. In the training set, we randomly pick 240 samples for each pathology to retrieve. This approach can ensure we get a maximum balanced sub-dataset containing 13230 patients' EHR in total. The random seed is set to 42.

B.3 Setup for Proactive Diagnostic Questioning Mechanism

We mask certain existing manifestations of a patient to simulate scenarios where they are missing. MedRAG then generates follow-up questions based on the remaining information. If MedRAG identifies the removed manifestations during questioning, they are added back to the patient's record, and diagnostic reasoning is repeated to evaluate the improvement in diagnostic accuracy.

We begin by selecting all matching manifestation nodes E_{L4d_s} and ranking them according to their discriminability scores. A proportion r of the nodes with the highest discriminability scores is then removed, simulating the scenario where certain key patient features are missing or unclear, shown in Equation 18. After removing, we match the removed nodes $E_{L4d_s}^{\text{del}}$ with each f_i , if the similarity score, the corresponding sentence f_i is also removed, as formalized in Equation 19, which simulates the loss of relevant patient information from the input.

$$e_{L4d_s}^{\text{del}} = \text{Top-}r(e_{L4d_s}, \sigma(e_{L4d_s})), \quad (18)$$

$$f_i^{\text{del}} = \bigcup_{f_i} \{f_i \mid S(f_i, e_{L4d_s}^{\text{del}}, \mathcal{E}) > t\}, \quad (19)$$

where $e_{L4d_s}^{\text{del}}$ represents the nodes removed from e_{L4d_s} based on the similarity score threshold t and f_i^{del} is removed f_i .

B.4 Prompt Engineering

The prompt configuration for disease clustering is shown below:

Cluster the following diseases into multiple categories based on the similarity of their manifestations, affected locations, and other characteristics. Diseases: {}.

The prompt configuration for the generative model in MedRAG is illustrated in Figure A1. The first block provides instructions as the system prompt. The second block displays the answer template. In the final block, relevant information including the patient's manifestations q , retrieved documents d_r , and diagnostic differences K , is populated in this field.

C Baseline Details

We conducted experiments on six baseline models and compared them with MedRAG.

- **Naive RAG + COT** [59] We apply the chain-of-thought (COT) prompting with a naive RAG model, which only retrieves documents without additional enhancements.
- **FL-RAG** [45] FL-RAG is a multi-round retrieval method that triggers the retrieval module every n tokens.
- **FS-RAG** [54] FS-RAG is an interleaving retrieval method that improves multi-round question answering by alternating between COT reasoning and document retrieval.
- **FLARE** [25] FLARE is an active RAG method that improves knowledge-intensive tasks by retrieving relevant documents when the model encounters uncertain tokens.
- **DRAGIN** [52] DRAGIN is a dynamic retrieval method that enhances language models by retrieving relevant documents based on real-time information needs during generation, triggered by token uncertainty.

Configuration	L1	L2	L3
w/ augmented feature node	79.25	75.47	67.92
w/o augmented feature node	66.04	60.38	49.06
w/ diagnostic key difference node	79.25	75.47	67.92
w/o diagnostic key difference node	77.36	71.70	64.15
w/ L2 & L3	79.25	75.47	67.92
w/o L2 & L3	63.64	57.58	51.52

Table A2: Impact of KG components on the performance of MedRAG

Models	BERTScore	BLEU	ROUGE	METEOR
FSRAG	0.7853	0.0963	0.1459	0.1490
FLARE	0.8328	0.1637	0.1011	0.1923
FL-RAG	0.8130	0.1551	0.2171	0.2054
Dragin	0.8259	0.2036	0.2053	0.2081
SRRAG	0.8346	0.2013	0.2722	0.2756
MedRAG	0.8359	0.2189	0.2863	0.2822

Table A1: Results of objective performance on CCPD

- **SR-RAG** [57] In SR-RAG, relevant passages are retrieved from an external corpus based on the initial query and then incorporated into the input of the language model

D Intermediate Results

D.1 Disease Clustering Result

The result of disease clustering in CPDD is Shown in Figure A2. Through the disease clustering operation, we group different forms and representations of the same disease in the EHR database together, assigning a topic to each cluster. This process unifies the representation of diseases, ensuring consistency and comparability. Additionally, it provides a unified foundation for subsequent disease knowledge graph construction and augmentation.

D.2 Example of Diagnostic Differences Knowledge Graph

While lumbar canal stenosis and sciatica share some similar features, the critical distinguishing factor lies in the response to sitting. In lumbar canal stenosis, features are typically alleviated when sitting, whereas in sciatica, sitting tends to exacerbate the discomfort. The augmented disease features are shown in Figure A3.

E Report Generation Evaluation

To evaluate the report generation of MedRAG, we conducted both objective and subjective evaluations on the generated reports of CCPD, since the DDXPlus dataset does not contain report data.

- **Objectice Evaluation:** We use BERTScore, BLEU, ROUGE, and METEOR as metrics. The result is shown in Table A1.
- **Subjective Evaluation:** Reports were generated for 10 randomly selected patients using SRRAG and MedRAG. The results were scored on 4 Mini-CEX criteria (Scale 1-9) [39],

and assessed by GPT-4o [50], with validation by doctors. The results were: SRRAG 277, MedRAG 290 out of 360.

F Ablation Study on KG Components

In order to evaluate how different components in diagnostic differences KG, we conducted extra ablation study focusing on key components. Specifically, we examined the effects of diagnostic key difference nodes, augmented feature nodes, patient clinical feature matching, and the augmentation of diagnostic differences.

Results in Table A2 show that KG components like diagnostic key difference nodes, augmented feature nodes, the patient clinical feature matching and the augmentation of diagnostic differences contribute to MedRAG’s overall effectiveness significantly. Moreover, the hierarchical structure of the constructed diagnostic differences KG directly impacts the experimental results as well.

G User Interface (UI)

This section introduces how our MedRAG can be integrated into the user interface design of the healthcare copilot system. The healthcare copilot offers three modes of interaction, as shown in Figure A4.

- **Consultation Mode:** By monitoring the consultation dialogue between the doctor and patient, the system extracts patient manifestations in real-time and provides diagnostic suggestions along with proactive questioning recommendations to guide the consultation.
- **EHR Mode:** By uploading the patient’s EHR to the healthcare copilot system, this system automatically extracts the relevant patient manifestations for diagnostic purposes.
- **Typewriting Mode:** The user can manually input the patient’s manifestations into the system.

On the results page shown in Figure A5, the output of the healthcare copilot system include diagnoses, instructive follow-up questions, physiotherapy treatments, and medication treatments. This UI integrates the most essential functions derived from extensive interviews we conducted with numerous healthcare practitioners. It ensures that the healthcare copilot system meets the practical needs of healthcare professionals, ultimately enhancing the overall quality of care.

H Future work

For future work, we aim to further enhance MedRAG’s capabilities by incorporating multimodal data, such as medical imaging (e.g., MRI), physiological signal data (e.g., ECG), and blood test data to improve diagnostic accuracy and broaden its applicability to a wider range of medical conditions. Additionally, we plan to deploy MedRAG within our healthcare copilot systems (The user interface is shown in the Appendix) for real-world hospital testing, ensuring its effectiveness in clinical settings. Furthermore, to improve usability for doctors, we will integrate a speech recognition module into the system. This feature will passively listen to conversations between doctors and patients during consultations without causing disruptions. Based on the dialogue content, it will provide real-time suggestions for follow-up questions and relevant explanations, assisting doctors in conducting more comprehensive and efficient patient assessments.

Variable	Definition
C	The clustering model
d_r	Retrieved relevant documents
D	Electronic Health Record (EHR) database
E_{L1}	The set of broad disease categories
E_{L2}	The set of disease subcategories
e_{L2_s}	The matched subcategory
E_{L3}	The set of specific disease names
$E_{L3_{raw}}$	the set of original disease descriptions in D
E_{L3_s}	The set of disease nodes connected with E_{L2_s}
E_{L4}	The set of disease-specific features
E_{L4_s}	The set of features nodes connected with node in E_{L3_s}
E_{del}	Deleted features in proactive diagnostic questioning
E_{L4a}	Disease-specific features augmented by the LLM
E_{L4d}	Features decomposed from the EHR database
$e_{L2_{ik}}$	The closest disease subcategory node
e_{Lij}	A disease or category name in the graph where $e_{Lij} \in E_{Li}$
f_i	A specific feature of the patient's manifestation
K	The set of diagnostic differences KG identified in the knowledge graph
p_a	Prompt used by \mathcal{M}_a for disease manifestation augmentation
p_{naive}	Simple prompt used by \mathcal{M}_g
p_s	Prompt designed for reasoning and generating diagnostic reports
P	The shortest path function
q	A input patient's manifestations
r	E_{L4_s} removing proportion in proactive diagnostic questioning mechanism
r_m	Relation type "has_manifestation_of" between diseases and their manifestations
r_s	Relation type "is_a" for hierarchical relationships
sim	The similarity score between patient features and nodes in the knowledge graph
T	Set of relevant matching nodes in the knowledge graph
t	Similarity score threshold in proactive diagnostic questioning mechanism
χ	The voting indicator function
δ	The matching filtering indicator function
\mathcal{E}	Embedding model used to compute similarity between features
\mathcal{G}	The four-tier hierarchical diagnostic knowledge graph
\mathcal{G}_D	The four-tier disease knowledge graph
\mathcal{M}_a	LLM used for disease manifestation augmentation
\mathcal{M}_g	LLM used for generating diagnostic reports
\mathcal{M}_h	LLM used for topic aggregation
S	The similarity model
ϕ	The decomposition function for q
$\sigma(e_{L4d_i})$	Discriminability score of a feature in the knowledge graph
Θ	The hierarchical aggregation operator

Table A3: List of variables and their definitions

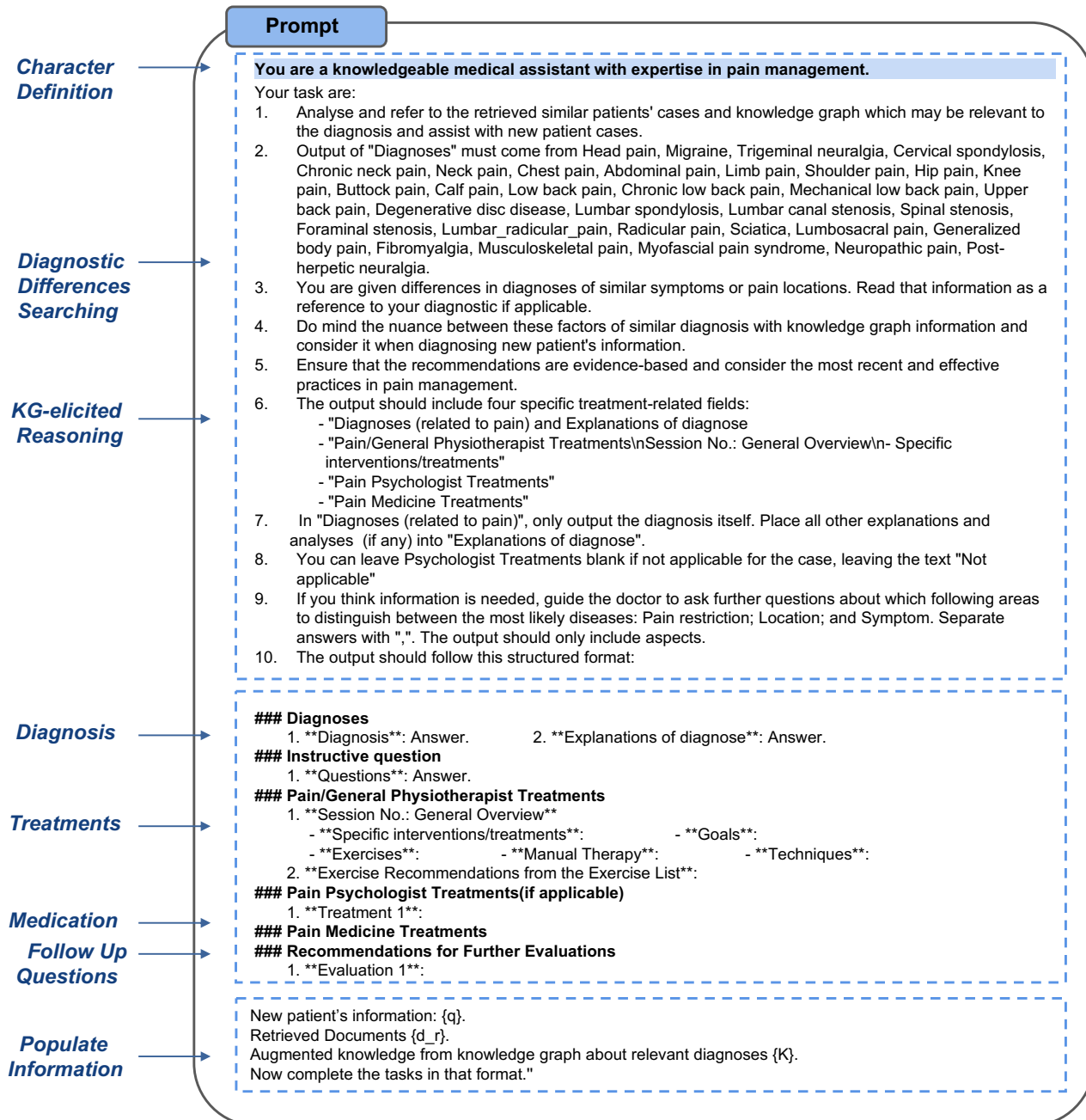


Figure A1: Prompt for the generative model of MedRAG

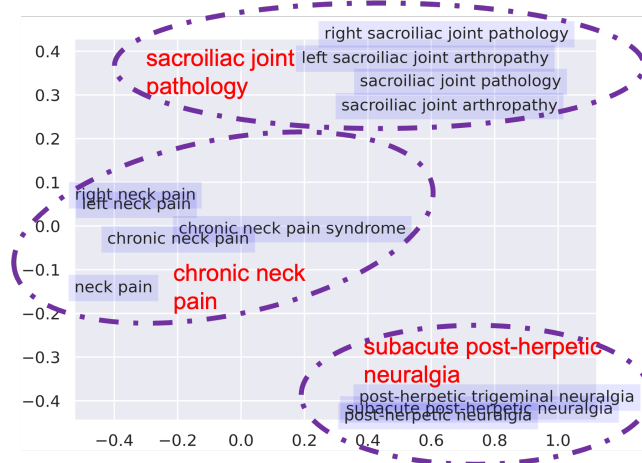


Figure A2: The result of disease clustering in CPDD

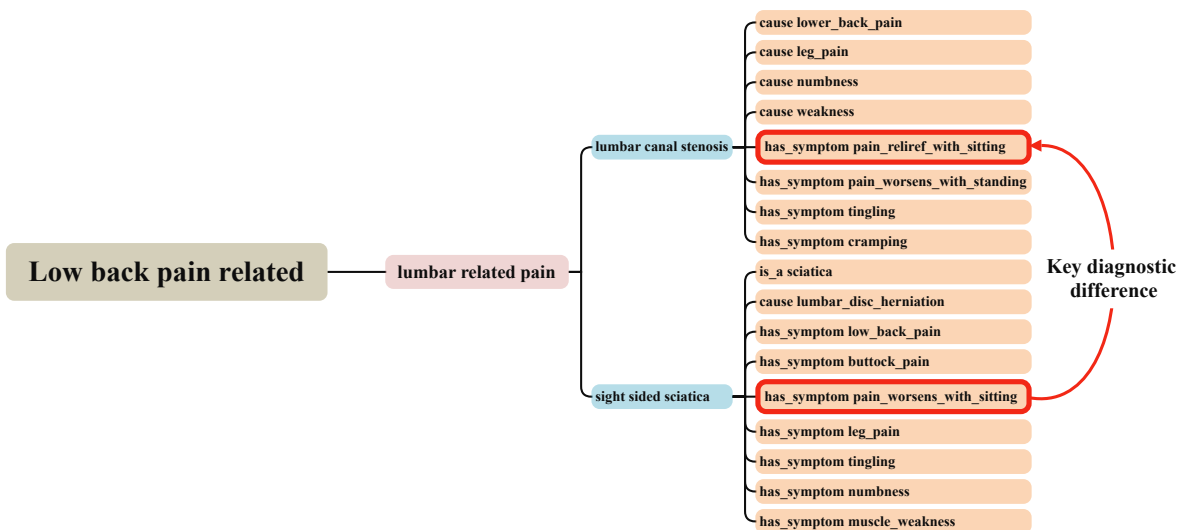


Figure A3: Diagnostic differences knowledge graph between lumbar canal stenosis and sciatica. (Similar manifestations but opposite responses to sitting (Alleviation vs. Exacerbation))

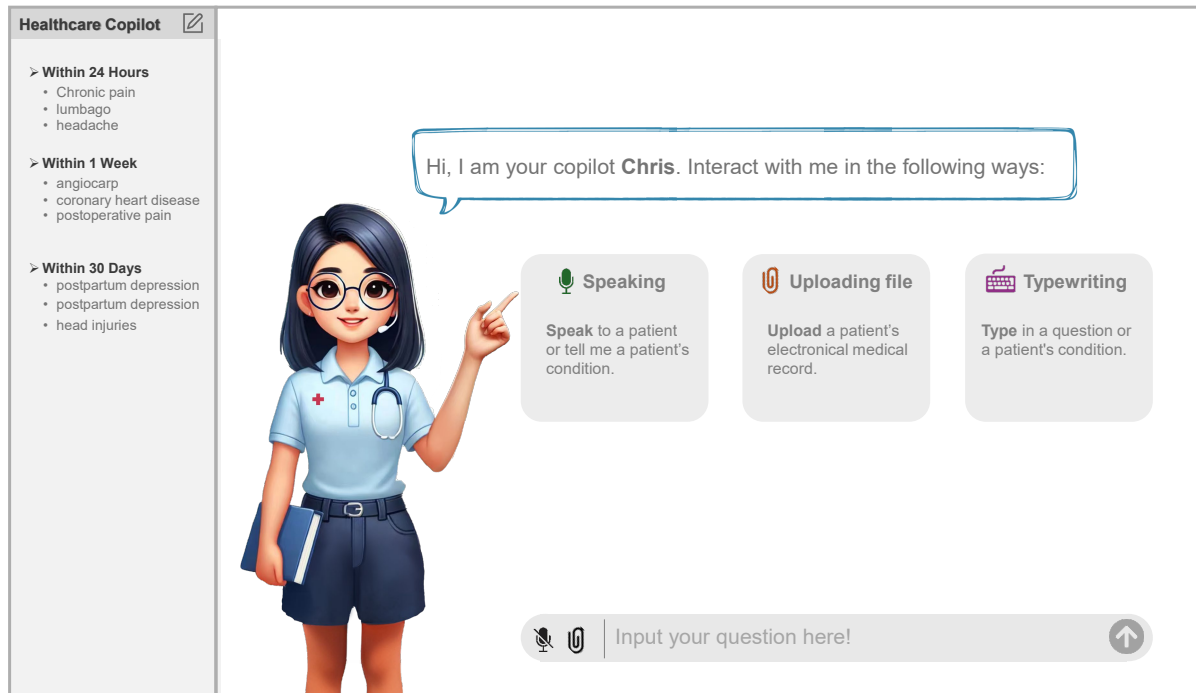


Figure A4: The interactive interface of healthcare copilot allows multi-turn medical Q&A through voice, files, and text.

This figure shows a specific interaction with the Healthcare Copilot for a patient with lumbar canal stenosis. The sidebar remains the same. In the main area, the user has input 'patient_501.json' and selected 'Me'. The copilot provides a detailed response:

- Diagnoses:**
 - Diagnosis: Lumbar canal stenosis
 - Explanations of diagnosis: The MRI findings indicate severe spinal canal stenosis at the L4/5 level leading to cauda equina compression. This can result in significant back and limb pain, as evidenced by the patient's symptoms of aching pain in the lower back with radiating pain down the [...].
- Instructive Follow-up Question:**
 - Does leaning forward or sitting relieve your pain?
- Pain/General Physiotherapist Treatments:**
 - **Specific interventions/treatments:** General physiotherapy focusing on patient education, [...].
 - **Goals:** To reduce pain levels, improve functional mobility, [...].
 - **Exercises:** Tailored exercises including back extensions, nerve glides, hamstring stretches, [...].
 - **Manual Therapy:** Techniques including Grade III mobilization of affected vertebral segments, [...].
 - **Techniques:** Application of hot packs for pain relief, pacing strategies in exercises, and [...].
- Pain Medicine Treatments:**
 - **Medicine:** The patient is advised to continue the usage of gabapentin and paracetamol as [...].

At the bottom is a text input field with icons for microphone, file, and up arrow, followed by the placeholder 'Input your question here!'. A small circular icon with an upward arrow is also present.

Figure A5: A specific example of how healthcare copilot could handle the diagnosis of lumbar canal stenosis using a JSON format medical record input, and output relevant treatments.